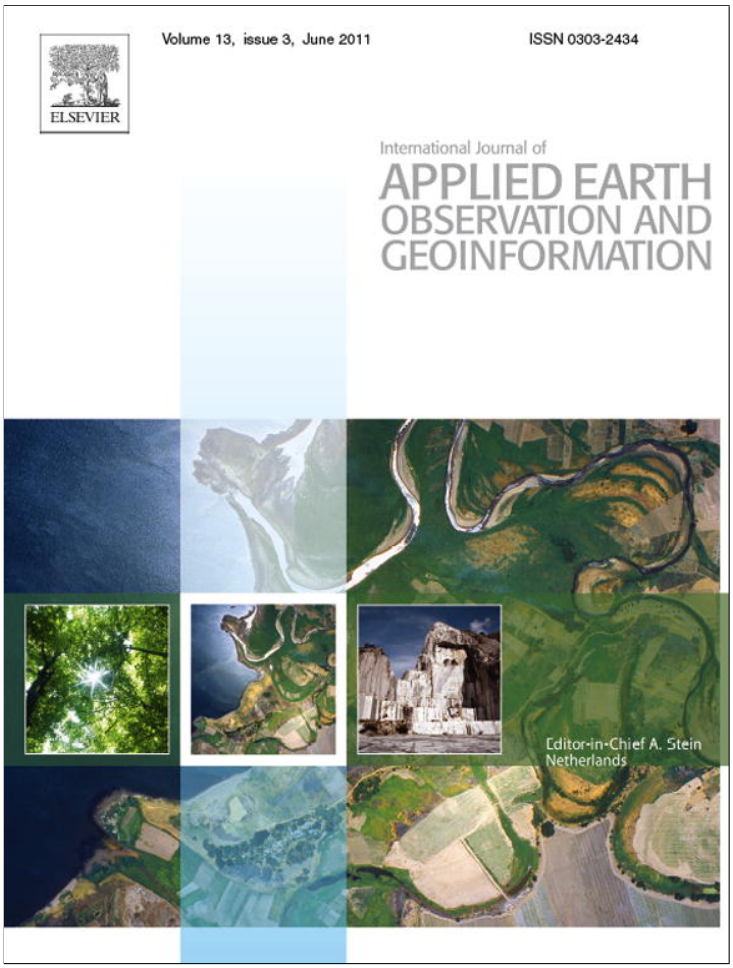

International Journal of Applied Earth Observation and Geoinformation 13 (2011) 409–419

Contents lists available at ScienceDirect

International Journal of Applied Earth Observation and Geoinformation

journal homepage: www.elsevier.com/locate/jag

A geostatistical approach to data harmonization – Application to radioactivity exposure data

O. Baume [a], J.O. Skøien [b], G.B.M. Heuvelink [a,*], E.J. Pebesma [c], S.J. Melles [a]

[a] Wageningen University, Department of Environmental Sciences, P.O. Box 47, 6700 AA Wageningen, The Netherlands
[b] Universiteit Utrecht, Department of Physical Geography, P.O. Box 80.115, 3508 TC Utrecht, The Netherlands
[c] Institute for Geoinformatics, University of Muenster, Weseler Strasse 253, D-48151 Muenster, Germany

ARTICLE INFO

Article history:
Received 8 April 2010
Accepted 1 September 2010

Keywords:
Network bias
Measurement equation
Natural drifts
Least squares estimation
Universal kriging

ABSTRACT

Environmental issues such as air, groundwater pollution and climate change are frequently studied at spatial scales that cross boundaries between political and administrative regions. It is common for different administrations to employ different data collection methods. If these differences are not taken into account in spatial interpolation procedures then biases may appear and cause unrealistic results. The resulting maps may show misleading patterns and lead to wrong interpretations. Also, errors will propagate when these maps are used as input to environmental process models. In this paper we present and apply a geostatistical model that generalizes the universal kriging model such that it can handle heterogeneous data sources. The associated best linear unbiased estimation and prediction (BLUE and BLUP) equations are presented and it is shown that these lead to harmonized maps from which estimated biases are removed. The methodology is illustrated with an example of country bias removal in a radioactivity exposure assessment for four European countries. The application also addresses multicollinearity problems in data harmonization, which arise when both artificial bias factors and natural drifts are present and cannot easily be distinguished. Solutions for handling multicollinearity are suggested and directions for further investigations proposed.

1. Introduction

Mapping environmental variables often requires assimilation of data from multiple sources. Ideally, these data are collected using the same, standardized methods in field and laboratory, irrespective of the source. However in practice, data are often collected in different ways, particularly when they come from different political or administrative regions. Hence, when data from different sources are used for mapping purposes, resultant maps may be affected by systematic differences between data collection protocols. Taking the development of national and regional radioactivity monitoring networks in the EU as an example, many different protocols were implemented, using different measurement devices, site conditions and data processing steps (Bossew et al., 2008). The problem of data source heterogeneity is obviously not restricted to radiation science, but concerns the environmental sciences in general. For instance, data harmonization is an important issue in vegetation science (e.g. Bartholomeus et al., 2008), marine science (e.g. Otuama and Hamre, 2007), forest science (e.g. Gold et al., 2006) and soil science (e.g. Prechtel et al., 2009).

It is well known that different protocols complicate the joint use of disparate datasets in statistical models (Gego et al., 2005; Herold et al., 2006), and that preprocessing is required before different datasets are merged. Standardization is the prevailing approach, as concluded in inter-comparison studies that examined field protocols in various environmental risk assessment fields (Wagner et al., 2001; Parr et al., 2002; Schröder et al., 2006). Standardization implies that all parties involved agree on the methods used for data collection. When standardization is unfeasible or has been only partly achieved, harmonization is a complementary procedure to correct the data after they have been collected. Harmonization can be viewed as a "bottom-up approach" that should result in a state of comparability between data from different sources (Köhl et al., 2000). Harmonization of different measurement techniques generally involves calibration models that include constant and random measurement errors (Osborne, 1991). Both components must be addressed. Furthermore, detailed information on data collection and measurement specifications such as meta-data in a GIS (Schröder et al., 2006) is of beneficial use in the development of a harmonization procedure.

The objective of this research is to address the harmonization problem by taking into account both random and systematic measurement errors in a geostatistical framework. The methodology is applied to the mapping of radioactivity exposure across Europe,

* Corresponding author. Tel.: +31 317482716; fax: +31 317419000.
E-mail address: gerard.heuvelink@wur.nl (G.B.M. Heuvelink).

0303-2434/$ – see front matter © 2010 Elsevier B.V. All rights reserved.
doi:10.1016/j.jag.2010.09.002

using data from the European-wide data exchange platform (EURDEP – http://eurdep.jrc.it/). The EURDEP data include measurement biases that may have several origins, such as differences in device type, site specifications and sampling protocols. As a result, the difference between two measurements at the same point in time at two different locations includes natural spatial variation in the phenomenon itself as well as systematic and random measurement errors. These errors should not appear in the final map as these will not reflect the true phenomenon of radioactivity dose rates.

The remainder of this paper is organized as follows. First, we introduce a statistical model in which measurements are a linear combination of the true state, a systematic measurement error, and a random error component. The state equation decomposes the true state into a structural part (e.g., the natural drift or trend) and a spatially correlated residual. Second, we describe the geostatistical harmonization procedure which optimally estimates the trend component and makes spatial predictions of the targeted environmental variable. Third, we illustrate the method with a real-world case study of mapping radioactivity exposure measures. We conclude with a discussion on the issue of multicollinearity between the bias and natural trend components and its influence on estimation precision, and a discussion on the future developments of our approach, which might generalize systematic harmonization procedures in geostatistical assessment studies.

2. Geostatistical formulation of the harmonization problem

When dealing with measured data of an environmental phenomenon in the context of random and systematic measurement errors, geostatistical model building requires three distinct steps. First, the phenomenon itself is modelled by defining a state equation that defines the relationship between the target variable and its covariates, and that includes a stochastic residual. The spatial dependence structure of the stochastic residual must also be described. Second, the relationship between the target variable and its measurement is described. Third, measurement biases are related to measurement artifacts. These three steps are described in the next subsections.

2.1. State equation

Consider a phenomenon z over a spatial domain $D \subset R^k$, $k \geq 2$ that we want to map. z is accessible at locations $\{\mathbf{s}_i \in D, i = 1, \ldots, n\}$. In geostatistics the values $\{z(\mathbf{s}_i)\}$ are treated as outcomes of a random field $\{Z(\mathbf{s}), \forall\, \mathbf{s} \in D\}$, which is characterized by a joint probability distribution. Commonly, Z is described as the sum of a mean function m and a stochastic residual δ, expressed as:

$$Z(\mathbf{s}) = m(\mathbf{s}) + \delta(\mathbf{s}). \tag{1}$$

The mean function m is known as the trend or drift; δ is a zero-mean error term, assumed intrinsically stationary. In many cases trend functions are described through a linear model (Chilès and Delfiner, 1999):

$$m(\mathbf{s}) = \mathbf{F_a}(\mathbf{s})\mathbf{a} + \mathbf{F}_{\boldsymbol{\alpha}}(\mathbf{s})\boldsymbol{\alpha}, \tag{2}$$

where $\mathbf{F}(\mathbf{s}) = [\mathbf{F_a}(\mathbf{s})\ \mathbf{F}_{\boldsymbol{\alpha}}(\mathbf{s})]$ is a vector of trend component values at location $\mathbf{s}$; $\mathbf{F_a}(\mathbf{s})$ represents the components for which associated parameter coefficients $\mathbf{a}$ are known; $\mathbf{F}_{\boldsymbol{\alpha}}(\mathbf{s})$ represents the vector of components for which coefficients $\boldsymbol{\alpha}$ must be estimated from the data.

In this setting the trend components may refer to both continuous and categorical explanatory variables that are traditionally included in external drift modelling. In the $\mathbf{F}(\mathbf{s})$ vector, the entry for each categorical independent variable is usually translated into as many binary dummy entries as there are categories, minus one (but see below for an alternative approach).

2.2. Measurement equation

The phenomenon modelled with the state variable z is only accessible through measurements $y(\mathbf{s}_i)$ at locations $\{\mathbf{s}_i \in D, i = 1, \ldots, n\}$. To distinguish between the true state and measurement of the true state, we define a measurement error term $e(\mathbf{s}_i)$ such that:

$$y(\mathbf{s}_i) = z(\mathbf{s}_i) + e(\mathbf{s}_i). \tag{3}$$

The exact values of the measurement errors $e(\mathbf{s}_i)$ are typically not known. However, the degree of variation in the random error component of e and the factors that impact measurement errors are often reasonably well known. Thus, the $e(\mathbf{s}_i)$ may be treated as outcomes of random variables whose probability distributions are known. Hence, we define random functions Y and ε over D, associated with both measured and measurement error variables. Often referred to as the measurement equation (e.g. Cressie, 1993), we write:

$$Y(\mathbf{s}_i) = Z(\mathbf{s}_i) + \varepsilon(\mathbf{s}_i). \tag{4}$$

2.3. Error equation

The measurement error $\varepsilon(\mathbf{s}_i)$ can be divided into systematic measurement errors (e.g. biases) and random measurement errors. As with natural drifts, some measurement biases may have a known value – the bias is valid for a certain type of sensor for instance. In the more usual case measurement biases will be unknown, but they can be related to specific factors, categories or time periods, and estimated from the data. In addition to systematic errors, we assume a random measurement error (Christensen, 1991; Marcotte, 1995). The multiple error components can be represented as follows:

$$\varepsilon(\mathbf{s}_i) = \mathbf{G_b}(\mathbf{s}_i)\mathbf{b} + \mathbf{G}_{\boldsymbol{\beta}}(\mathbf{s}_i)\boldsymbol{\beta} + \zeta(\mathbf{s}_i), \tag{5}$$

where $\mathbf{G}(\mathbf{s}_i) = [\mathbf{G_b}(\mathbf{s}_i)\ \mathbf{G}_{\beta}(\mathbf{s}_i)]$ is a vector of measurement biases at location $\mathbf{s}_i$; $\mathbf{G}_b(\mathbf{s}_i)$ represents bias factors for which we know the coefficients $\mathbf{b}$; $\mathbf{G}_{\beta}(\mathbf{s}_i)$ stands for bias factors whose coefficients $\boldsymbol{\beta}$ must be estimated. ζ is a zero-mean random measurement error component.

2.4. Harmonization model

We define a harmonization model at measurement locations $\mathbf{s}_i$ combining Eqs. (1), (2), (4) and (5):

$$\begin{cases} \mathbf{Z} = \mathbf{F}_a\mathbf{a} + \mathbf{F}_{\alpha}\boldsymbol{\alpha} + \boldsymbol{\delta}, \\ \mathbf{Y} = \mathbf{Z} + \boldsymbol{\varepsilon}, \\ \boldsymbol{\varepsilon} = \mathbf{G}_b\mathbf{b} + \mathbf{G}_{\beta}\boldsymbol{\beta} + \boldsymbol{\zeta}. \end{cases} \tag{6}$$

To complete the definition of the geostatistical harmonization model we assume that the stochastic residual $\boldsymbol{\delta}$ and random measurement error $\boldsymbol{\zeta}$ are normally distributed and mutually uncorrelated. The variance–covariance matrices of $\boldsymbol{\delta}$ and $\boldsymbol{\zeta}$ at the n observation locations are denoted as:

$$\begin{cases} \mathbf{V} = Var(\boldsymbol{\delta}), \\ \mathbf{W} = Var(\boldsymbol{\zeta}). \end{cases} \tag{7}$$

3. Best linear unbiased estimation and prediction in the heterogeneous case

In order to predict Z at unmeasured locations, we compute the conditional distribution of Z at location $\mathbf{s}_{n+1}$ given observations

$y(\mathbf{s}_i)$:

$$F_Z(z;\mathbf{s}_{n+1}) = P(Z(\mathbf{s}_{n+1}) \le z | y(\mathbf{s}_i), \quad i = 1,\ldots,n). \tag{8}$$

We first separate out the known part of the drift in Eq. (6):

$$\mathbf{Y} - (\mathbf{F}_a\mathbf{a} + \mathbf{G}_b\mathbf{b}) = \mathbf{F}_\alpha\boldsymbol{\alpha} + \mathbf{G}_\beta\boldsymbol{\beta} + \boldsymbol{\delta} + \boldsymbol{\zeta}. \tag{9}$$

Defining $\mathbf{U} = \mathbf{Y} - (\mathbf{F}_a\mathbf{a} + \mathbf{G}_b\mathbf{b})$ and $\boldsymbol{\phi} = \boldsymbol{\delta} + \boldsymbol{\zeta}$ leads to:

$$\mathbf{U} = \mathbf{X}\boldsymbol{\theta} + \boldsymbol{\phi}, \tag{10}$$

where

$$\mathbf{X} = [\mathbf{F}_\alpha \ \ \mathbf{G}_\beta] \text{ and } \boldsymbol{\theta} = \begin{bmatrix} \boldsymbol{\alpha} \\ \boldsymbol{\beta} \end{bmatrix}.$$

The statistical moments of $\mathbf{U}$ satisfy:

$$\begin{cases} E(\mathbf{U}) = \mathbf{X}\boldsymbol{\theta}, \\ Var(\mathbf{U}) = \mathbf{V} + \mathbf{W}. \end{cases} \tag{11}$$

3.1. Best linear unbiased estimation of $\boldsymbol{\theta}$

Estimation of $\boldsymbol{\theta}$ from the observations that satisfy Eq. (10) is a classical problem of multiple linear regression. We estimate the parameters $\boldsymbol{\theta}$ in the same manner as Christensen (1991),

$$\begin{cases} \hat{\boldsymbol{\theta}} = \begin{bmatrix} \hat{\boldsymbol{\alpha}} \\ \hat{\boldsymbol{\beta}} \end{bmatrix} = (\mathbf{X}'(\mathbf{V}+\mathbf{W})^{-1}\mathbf{X})^{-1}\mathbf{X}'(\mathbf{V}+\mathbf{W})^{-1}\mathbf{U}, \\ Var(\hat{\boldsymbol{\theta}}) = (\mathbf{X}'(\mathbf{V}+\mathbf{W})^{-1}\mathbf{X})^{-1}. \end{cases} \tag{12}$$

The $'$ indicates the transposition operator. This solution is the best linear unbiased estimate (BLUE) with the smallest estimation error variance. In cases where one or more covariates of Eq.(10) are categorical, the traditional approach to avoiding multicollinearity in dummy variables is to delete redundant categories from each categorical variable (Searle, 1997). An alternative approach is to impose the constraint that the dummy parameters for each categorical covariate sum to zero (Suits, 1957). This simplifies interpretation of the estimated parameters, which is particularly useful in cases where the regression equation contains several categorical variables.

3.2. Identification of variance–covariance matrices

The covariance matrix of random measurement errors $\mathbf{W}$ may be based on repeated measurements using the same device or based on expert knowledge. Assuming that random measurement errors have constant variance and are mutually independent, $\mathbf{W}$ is a diagonal matrix $\mathbf{W} = \sigma_M^2\mathbf{I}$, where σ_M^2 is the variance of the measurement errors. The assumption of constant measurement error variance is implausible if different device types have different measurement errors, or if the measurement locations differ in their level of compliance with site specifications (Zähringer and Sempau, 1996; Bossew et al., 2008). In such a case it is more realistic to consider that $\mathbf{W}$ bears individual measurement error variances along its diagonal.

Estimation of the stochastic residual covariance matrix $\mathbf{V}$ is hampered by the fact that estimation of $\mathbf{V}$ requires the model coefficients $\boldsymbol{\theta}$ to be known, while estimation of $\boldsymbol{\theta}$ requires $\mathbf{V}$ as in Eq. (12). This "chicken and egg" problem (Armstrong, 1984) can be solved using an iterative procedure. The first estimate of $\boldsymbol{\theta}$ is carried out with ordinary least squares (OLS), which is equivalent to substituting $\mathbf{V}$ with the identity matrix $\mathbf{I}$. Residuals can then be computed and serve as an initial data set for estimation of $\mathbf{V}$. This estimate is then used to re-compute preliminary generalized least squares (GLS) estimates for $\boldsymbol{\theta}$. Repeated iteration yields new estimates of both $\boldsymbol{\theta}$ and $\mathbf{V}$ until convergence.

3.3. Best linear unbiased prediction of $\mathbf{Z}$

After BLUE estimates of model parameters

$$\boldsymbol{\theta} = \begin{bmatrix} \boldsymbol{\alpha} \\ \boldsymbol{\beta} \end{bmatrix},$$

are computed, we proceed to spatial prediction by applying kriging, also known as best linear unbiased prediction (BLUP). Because the system is normally distributed, optimal prediction of the process at an unobserved location is linear in the observations, which can be expressed as:

$$\hat{Z}(\mathbf{s}_{n+1}) = p + \mathbf{F}_a(\mathbf{s}_{n+1})\mathbf{a} + \mathbf{F}_\alpha(\mathbf{s}_{n+1})\hat{\boldsymbol{\alpha}} + \mathbf{q}'(\mathbf{Y} - \mathbf{F}_a\mathbf{a} - \mathbf{F}_\alpha\hat{\boldsymbol{\alpha}} - \mathbf{G}_b\mathbf{b} - \mathbf{G}_\beta\hat{\boldsymbol{\beta}}), \tag{13}$$

where the known and estimated biases have been subtracted from the measurement vector because these affect the measurements but not the true state of the process. The scalar p and the vector $\mathbf{q}$ must be chosen such that the three key properties of BLUP (i.e. best, linear and unbiased) are satisfied.

Linearity is a property of the predictor by construction. Unbiasedness requires that:

$$E[\hat{Z}(\mathbf{s}_{n+1})] = E[Z(\mathbf{s}_{n+1})]. \tag{14}$$

Evaluating the expected values leads to:

$$\begin{aligned} &p + \mathbf{F}_a(\mathbf{s}_{n+1})\mathbf{a} + \mathbf{F}_\alpha(\mathbf{s}_{n+1})E[\hat{\boldsymbol{\alpha}}] \\ &\quad + \mathbf{q}'(E[\mathbf{Y}] - \mathbf{F}_a\mathbf{a} - \mathbf{F}_\alpha E[\hat{\boldsymbol{\alpha}}] - \mathbf{G}_b\mathbf{b} - \mathbf{G}_\beta E[\hat{\boldsymbol{\beta}}]) \\ &= \mathbf{F}_a(\mathbf{s}_{n+1})\mathbf{a} + \mathbf{F}_\alpha(\mathbf{s}_{n+1})\boldsymbol{\alpha}. \end{aligned} \tag{15}$$

From the BLUE expression properties, we have $E[\hat{\boldsymbol{\alpha}}] = \boldsymbol{\alpha}$ and $E[\hat{\boldsymbol{\beta}}] = \boldsymbol{\beta}$, and from the model definition $E[\mathbf{Y}] = \mathbf{F}_a\mathbf{a} + \mathbf{F}_\alpha\boldsymbol{\alpha} + \mathbf{G}_b\mathbf{b} + \mathbf{G}_\beta\boldsymbol{\beta}$. Hence,

$$E[\mathbf{Y}] - \mathbf{F}_a\mathbf{a} - \mathbf{F}_\alpha\boldsymbol{\alpha} - \mathbf{G}_b\mathbf{b} - \mathbf{G}_\beta\boldsymbol{\beta} = 0, \tag{16}$$

so that

$$p = 0. \tag{17}$$

The kriging variance is given by the quadratic form:

$$E[(\hat{Z}(\mathbf{s}_{n+1}) - Z(\mathbf{s}_{n+1}))^2] = E[(c + \mathbf{q}'\mathbf{d})^2], \tag{18}$$

where c and $\mathbf{d}$ are given by:

$$\begin{cases} c = \mathbf{F}_\alpha(\mathbf{s}_{n+1})(\hat{\boldsymbol{\alpha}} - \boldsymbol{\alpha}) + \delta(\mathbf{s}_{n+1}), \\ \mathbf{d} = \mathbf{X}(\theta - \hat{\theta}) + \boldsymbol{\phi}. \end{cases} \tag{19}$$

Minimizing the kriging variance by setting the derivative of Eq. (18) with respect to $\mathbf{q}$ to zero gives:

$$E[\mathbf{d}'\mathbf{d}]\mathbf{q} + E[c\,\mathbf{d}] = 0. \tag{20}$$

Substituting c and $\mathbf{d}$ and the estimates from Eq. (12) yields:

$$\begin{aligned} &[\mathbf{X}(\mathbf{X}'(\mathbf{V}+\mathbf{W})^{-1}\mathbf{X})^{-1}\mathbf{X}' - (\mathbf{V}+\mathbf{W})]\mathbf{q} \\ &\quad = [\mathbf{X}(\mathbf{X}'(\mathbf{V}+\mathbf{W})^{-1}\mathbf{X})^{-1}\mathbf{X}' - (\mathbf{V}+\mathbf{W})](\mathbf{V}+\mathbf{W})^{-1}Cov(\boldsymbol{\delta}, \delta(\mathbf{s}_{n+1})). \end{aligned} \tag{21}$$

Hence $\mathbf{q} = (\mathbf{V}+\mathbf{W})^{-1}\mathbf{v}'_{n+1}$, with $\mathbf{v}_{n+1} = Cov(\delta(\mathbf{s}_{n+1}), \boldsymbol{\delta})$. As a result the harmonized BLUP prediction of Z is:

$$\hat{Z}(\mathbf{s}_{n+1}) = \mathbf{F}(\mathbf{s}_{n+1})\begin{bmatrix} \mathbf{a} \\ \hat{\boldsymbol{\alpha}} \end{bmatrix} + (\mathbf{V}+\mathbf{W})^{-1}\mathbf{v}'_{n+1}\left(\mathbf{Y} - \mathbf{F}\begin{bmatrix} \mathbf{a} \\ \hat{\boldsymbol{\alpha}} \end{bmatrix} - \mathbf{G}\begin{bmatrix} \mathbf{b} \\ \hat{\boldsymbol{\beta}} \end{bmatrix}\right). \tag{22}$$

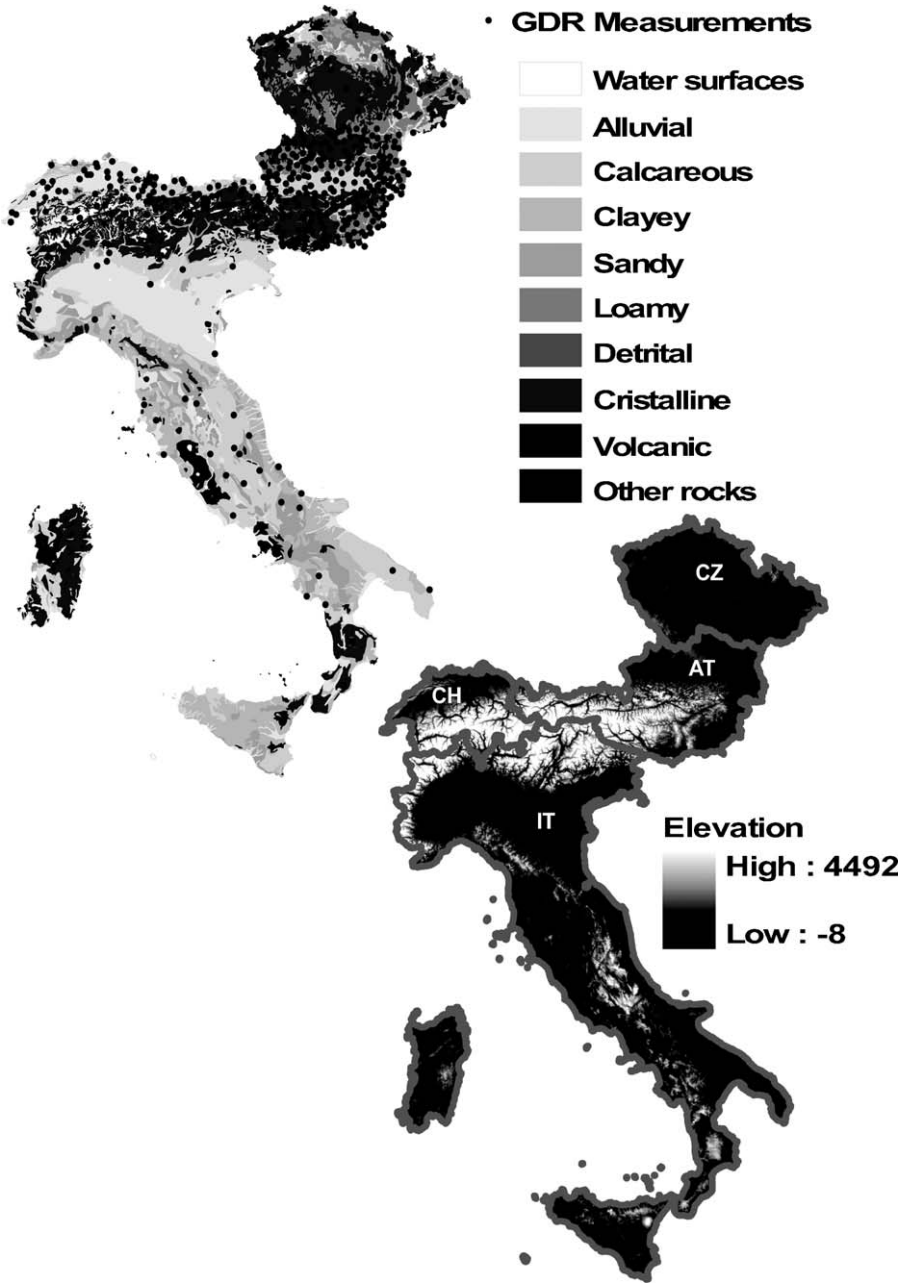

Fig. 1. External drifts of background gamma dose rates (GDR). Top map: soil map with GDR measurement locations. Bottom map: elevation with country borders.

The prediction result (Eq. (22)) has two terms. The first corresponds to the trend value of the state variable $Z(\mathbf{s}_{n+1})$. The second term is the interpolated residual, computed from the measurements. Note the differences with classical kriging – i.e. the homogeneous case where all data are from the same network and $\mathbf{G} \equiv 0$ and $\mathbf{W} \equiv 0$.

The prediction error variance associated with the predictor is given by:

$$Var(Z(\mathbf{s}_{n+1}) - \hat{Z}(\mathbf{s}_{n+1})) = Var(Z(\mathbf{s}_{n+1})) - 2\boldsymbol{\Lambda}'\mathbf{v}_{n+1} + \boldsymbol{\Lambda}'(\mathbf{V}+\mathbf{W})\boldsymbol{\Lambda}, \tag{23}$$

where

$$\boldsymbol{\Lambda}' = \mathbf{F}_\alpha(\mathbf{s}_{n+1})(\mathbf{F}'_\alpha(\mathbf{V}+\mathbf{W})^{-1}\mathbf{F}_\alpha)^{-1}\mathbf{F}'_\alpha(\mathbf{V}+\mathbf{W})^{-1} + \mathbf{q}'(\mathbf{I} - \mathbf{X}(\mathbf{X}'(\mathbf{V}+\mathbf{W})^{-1}\mathbf{X})^{-1}\mathbf{X}'(\mathbf{V}+\mathbf{W})^{-1}).$$

As can be seen from the BLUE expression (Eq. (12)), the drifts and heterogeneities are estimated from the overall covariance matrix ($\mathbf{V}+\mathbf{W}$). However, the prediction takes the overall (co)variance of the process only partially into account. In particular, the kriging weights $\mathbf{q}$ include only the covariance of the state variable $Cov(\delta(\mathbf{s}_{n+1}), \boldsymbol{\delta})$. If the variance of the random measurement error component is large, this will decrease $\mathbf{q}$ and result in a prediction value that is closer to the trend.

4. Real world example – mapping gamma dose rate at the European scale

Since the Chernobyl release in 1986, European countries have set up various networks to assess radioactivity levels and to design early warning systems. These national networks are heterogeneous in terms of density, design, and data handling. At the continen-

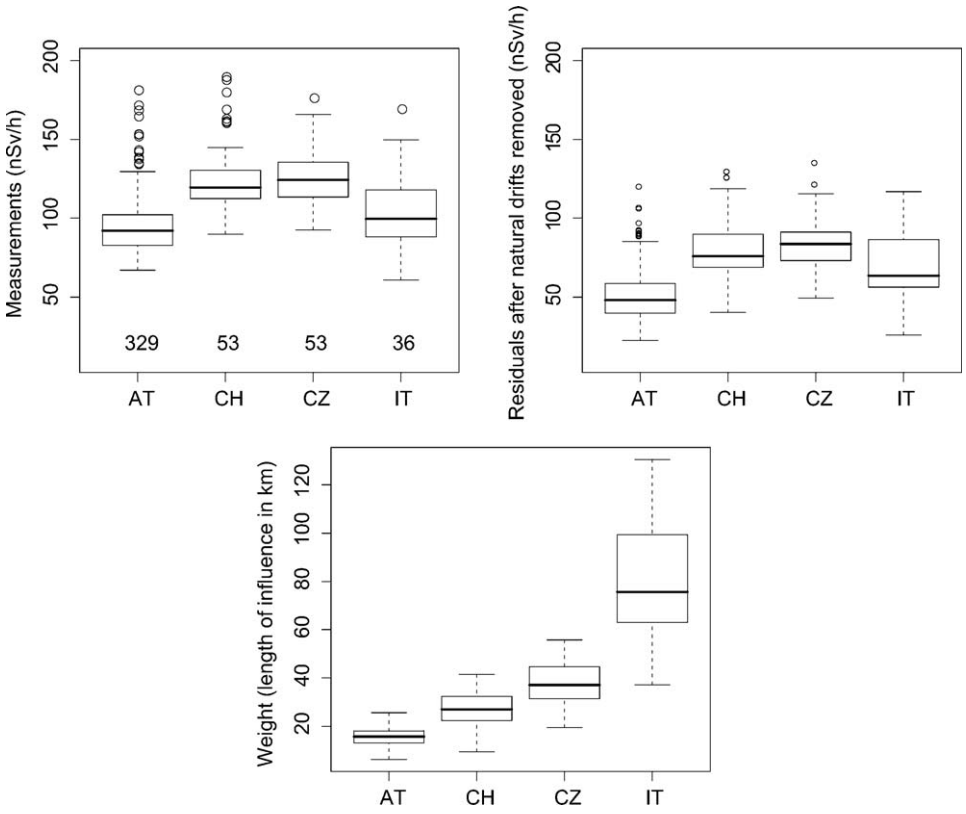

Fig. 2. Gamma dose rate (GDR) from EURDEP data (monthly average in December 2006) Top left: distribution of observed GDR versus country code. Top right: distribution of residuals (after natural drifts were removed) versus country code. Bottom: distribution of variogram estimation weights versus country code.

tal scale initiative was taken to centralize these national databases in the form of the European Radiological Data Exchange Platform (EURDEP) (De Cort and De Vries, 1997). The goal of this database is to provide data for routine and alert modes. The routine mode assesses background radioactivity levels. Alert mode is used to detect an unexpected release of radioactivity within a given amount of time. Data harmonization in an alert setting is beyond the scope of this paper as we focus on background monitoring of environmental data in the general case.

Background radioactivity comes from a combination of different sources. In our example application, we deal with gamma dose rate (GDR) measurements. GDR measurements integrate radioactive decay products over a wide variety of nuclides and GDR is therefore equivalent to a global measure of radioactivity. The common physical unit for GDR over time is nSv/h (nano Sievert per hour). The main factors to be accounted for are terrestrial radiation, cosmic radiation, and atmospheric washout from rainfall events. In a background situation, observations can be significantly affected by a variety of measurement biases related to site specification, device type, data handling, and the general standards employed individually by countries and regional networks. Thus it is necessary to harmonize the data when mapping radioactivity exposure at a European scale.

4.1. Filtering a country membership effect

We refer to Szegvary et al. (2007) for more details on radioactivity measurements in general and Bossew et al. (2008) for a detailed inventory of heterogeneity sources. Despite extensive efforts to describe and eliminate differences between networks, there are

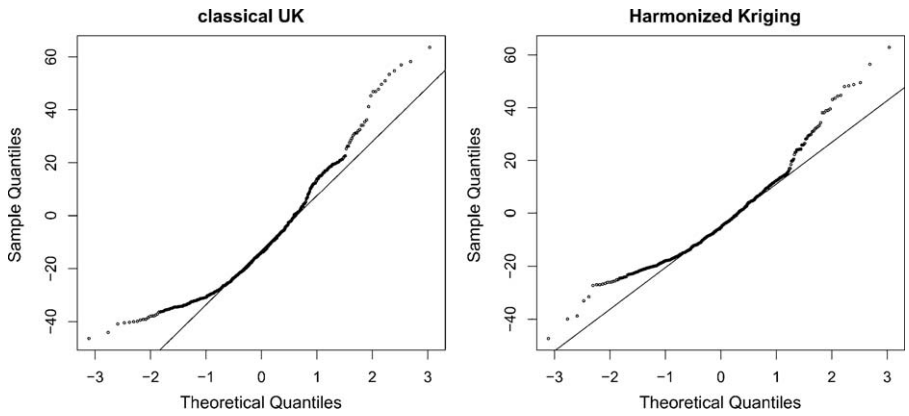

Fig. 3. Gamma dose rate (GDR) from EURDEP data (monthly average in December 2006): quantile–quantile plot of the residuals of the linear model – Classical UK (left) and Harmonized Kriging (right) against the normal distribution.

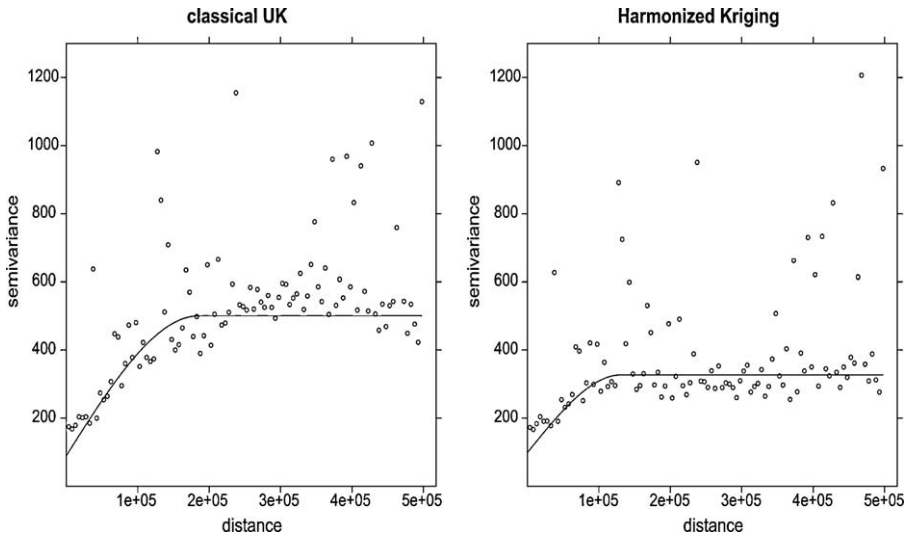

Fig. 4. Gamma dose rate (GDR) from EURDEP data (monthly average in December 2006): sample variogram of the residuals: Classical UK model (left) and Harmonized Kriging model (right).

still heterogeneities unaccounted for. For example, one source of heterogeneity is the so-called inherent background or self-effect of the probe, which refers to the radiation value that the probe reports when the true radiation is in fact zero. Self-effects depend on probe type and manufacturer, and although this source of heterogeneity may account for a high percentage of measured background GDR, self-effect data are not available for all countries.

We map GDR in four countries – Austria (AT), the Czech Republic (CZ), Italy (IT) and Switzerland (CH), based on monthly observations reported in the EURDEP database. In total, there are 471 measurement locations contained within these four countries. We assume that all network heterogeneities can be explained by country membership given that measurement devices are typically standardized within individual countries. In this case, the artefact of heterogeneity appears as a single factor: the country code. Country code is an indicator of bias in the data, although for instance, device type and site specification both have a large impact as well and should be distinguished in the analysis. As mentioned, a substantial part of the bias caused by device type and site specification will be captured by country code as most countries have standardized their internal procedures.

4.2. Harmonization model of EURDEP data

True background GDR is represented by a state equation that accounts for two natural drifts: soil type and cosmic radiation. Soil type is an important factor because it accounts for differences in terrestrial radioactivity and monthly temporal interactions with rainfall washout effects. Cosmic radiation depends on air pressure and altitude and can be accurately described by a physically-based deterministic model. A recent German study reported the statistical relationship between altitude above sea level and cosmic radiation, using airborne measurements (Wissmann et al., 2007). We will use their empirical model to estimate elevational differences in cosmic radiation as follows:

$$F_{\text{Elevation}}(h) = 6.22\exp(-0.001051\ \ h) + 26.91\exp(0.0004103\ \ h), \tag{24}$$

expressed in nSv/h and where elevation h is measured in meters. This formula applies to a certain type of gamma dose rate probe only (the Geiger–Müller GS05, largely used in Germany). For other device types, other empirical models were developed (Szegvary et al., 2007).

Table 1
Estimate and standard deviation of parameters (nSv/h) for Classical UK and Harmonized Kriging – n represents the number of measurements in each class.

	Classical UK		Harmonized Kriging		n
	Estimate	Std. dev.	Estimate	Std. dev.	
Austria (AT)	–	–	−17.5	3.2	329
Switzerland (CH)	–	–	8.9	4.1	53
Czech Republic (CZ)	–	–	7.2	3.9	53
Italy (IT)	–	–	1.4	3.7	36
Water surface and glacier	−0.7	5.2	−2.1	3.9	23
Alluvial deposits	3.2	4.1	2.1	2.6	94
Calcareous rocks	−0.2	4.2	−0.6	2.7	80
Clayey materials	−19.3	10.2	−20.6	8.7	4
Sandy materials	−5.2	7.1	−6.4	5.9	11
Loamy materials	4.3	4.2	4.4	2.5	113
Detrital formations	1.9	10.8	5.7	9.3	3
Crystalline rocks	8.2	4.2	9.3	2.6	109
Volcanic rocks	9.8	4.9	10.6	3.5	31
Other rocks	−1.9	10.2	−2.3	8.8	3
Intercept	69.9	–	72.0	2.9	471

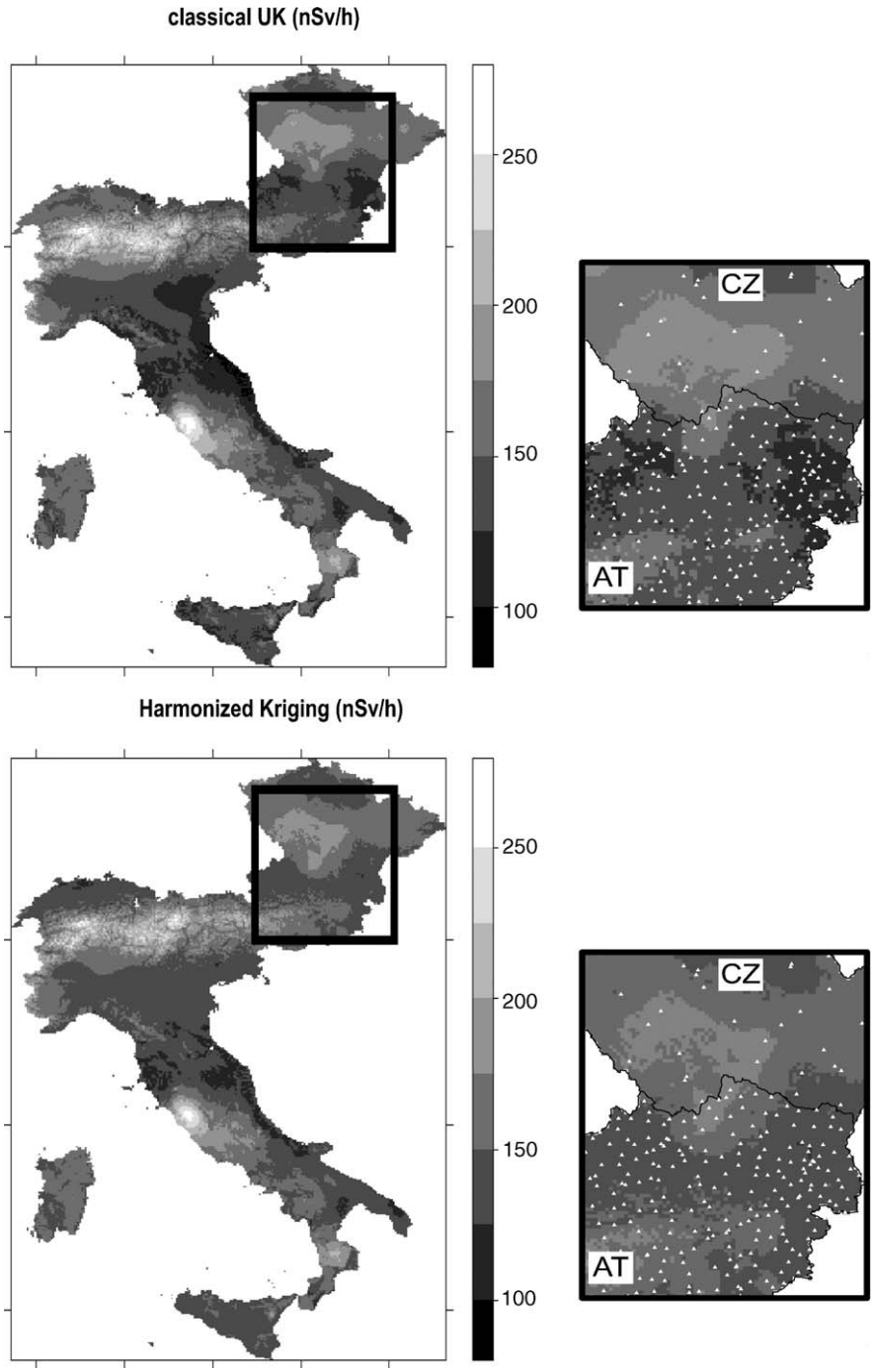

Fig. 5. Gamma dose rate (GDR) from EURDEP data (monthly average in December 2006): maps applying Classical UK (top) and Harmonized Kriging (bottom). Right hand panels show an enlarged portion of the Austrian–Czech border with measurement locations.

Soil effects are included in the trend model as a set of categorical dummy covariates. The effect of soil on GDR is not adequately known although Hiemstra et al. (2009) examined the effect of soil on GDR at a national scale in the Netherlands. The soil classification we use is extracted from the European soil database and describes only 10 soil classes (http://eusoils.jrc.it/ESDB_Archive/ESDBv2/). Fig. 1 presents the soil and elevation maps that are included as natural drifts in the model.

In this paper we analyze monthly GDR averages in the EURDEP database for December, 2006. This implies that we study background situations where meteorology has an average influence on the spatial variation of radioactivity exposure. Thus we assumed only two natural covariates of GDR implemented in the following model:

$$\begin{cases} \mathbf{U} = \mathbf{Y} - \mathbf{F}_{\text{Elevation}} \cdot 1, \\ \mathbf{U} = \mathbf{F}_{\text{Soil}}\, \boldsymbol{\alpha}_{\text{Soil}} + \mathbf{G}_{\text{Country}}\, \boldsymbol{\beta}_{\text{Country}} + \boldsymbol{\phi}, \end{cases} \tag{25}$$

following the notation in Sections 2 and 3.

The spatial density of EURDEP monitoring stations varies greatly between countries. This highly affects the efficiency of variogram estimation because the sample variogram is dominated by observations from countries with a dense network. Therefore we computed a robust weighted form of the variogram of residuals. At each

iteration in the estimation procedure for $\boldsymbol{\alpha}_{\text{Soil}}$ and $\boldsymbol{\beta}_{\text{Country}}$, the variogram was computed with a formulation as suggested by Rivoirard et al. (2000). Introducing a weight w_i associated with the residual values $\phi(\mathbf{s}_i)$ at measurement locations $\mathbf{s}_i$, the sample variogram is estimated as:

$$\gamma_w(h) = \frac{1}{2N(h)} \frac{\sum_{h-\delta h<|\mathbf{s}_i-\mathbf{s}_j|<h+\delta h} w_i w_j |\phi(\mathbf{s}_i)-\phi(\mathbf{s}_j)|^2}{\sum_{h-\delta h<|\mathbf{s}_i-\mathbf{s}_j|<h+\delta h} w_i w_j}. \quad (26)$$

Weights were computed by constructing Voronoï polygons of the measurements using an established method for mapping clustered data (Kovitz and Christakos, 2004). Each polygon corresponds to the measurement's area of influence. We chose the square root of polygon areas as weights $\{w_i\}$ in Eq. (26). Hence in our case weights characterize the influence length of measurements. An exception was made for the islands of Sardegna and Sicily. These islands were excluded from the computation of Voronoï weights because they had a sizable impact despite being isolated from existing measurements in the data set. Note that the weighted formulation for variogram calculation reduces the dominant influence of densely sampled areas, but that at short lags, where no point pairs from sparsely sampled areas are available, the variogram values will still be determined by the densely sampled areas only.

Boxplots shown in Fig. 2 demonstrate a clear discrepancy between countries in background GDR values, which was not substantially reduced by removal of the natural drifts (compare top left and top right plots). For example, Austria and Switzerland have similar soil types and elevational ranges but their mean GDR values differ by 31 nSv/h, which indicates a clear bias between these two countries. The boxplot of computed variogram estimation weights (Fig. 2, bottom) confirms that these national networks have largely different sampling densities. Austria has the densest network while Italy has the sparsest.

Random measurement error for GDR monitors is typically in the vicinity of 5 nSv/h (Bossew et al., 2008). Therefore, we assume in this example that $\mathbf{W}$ is a diagonal matrix $\sigma_M^2\mathbf{I}$ with $\sigma_M^2 = 25\,(\text{nSv/h})^2$.

5. Results: Harmonized Kriging

We estimated country biases and applied data harmonization while interpolating GDR for the four countries. Results from harmonization are referred to as Harmonized Kriging. We compared Harmonized Kriging with the classical case where constant country biases are not considered or included in the universal kriging model. These results are referred to as Classical UK. We used all 471 observations for estimation of the model parameters and simultaneous kriging of residuals.

The statistical distribution of the residuals from the linear model is compared in Fig. 3 to theoretical normal distributions in the form of quantile–quantile plots. The left panel shows the residuals from the model without harmonization, whereas the right panel shows residuals of the model including country bias estimation. Harmonization leads to a more symmetric distribution, although deviation from normality still occurs at the tails of the distribution.

Final weighted sample variograms of the residuals are shown for comparison purposes in Fig. 4. On the left is the weighted variogram without harmonization, and the right depicts the Harmonized Kriging variogram. The lag size used to calculate the sample variograms was 5 km. Spherical variograms were fitted to the sample variograms using a weighted least squares criterion, with weights proportional to the number of point pairs within the lag. A decrease in both sill (from 413 to 229 $(\text{nSv/h})^2$) and range (from 186 to 132 km) was observed when country bias was introduced in the model (from left to right). As a result the harmonization procedure reduced the sill-to-nugget ratio from 4.2 to 1.9.

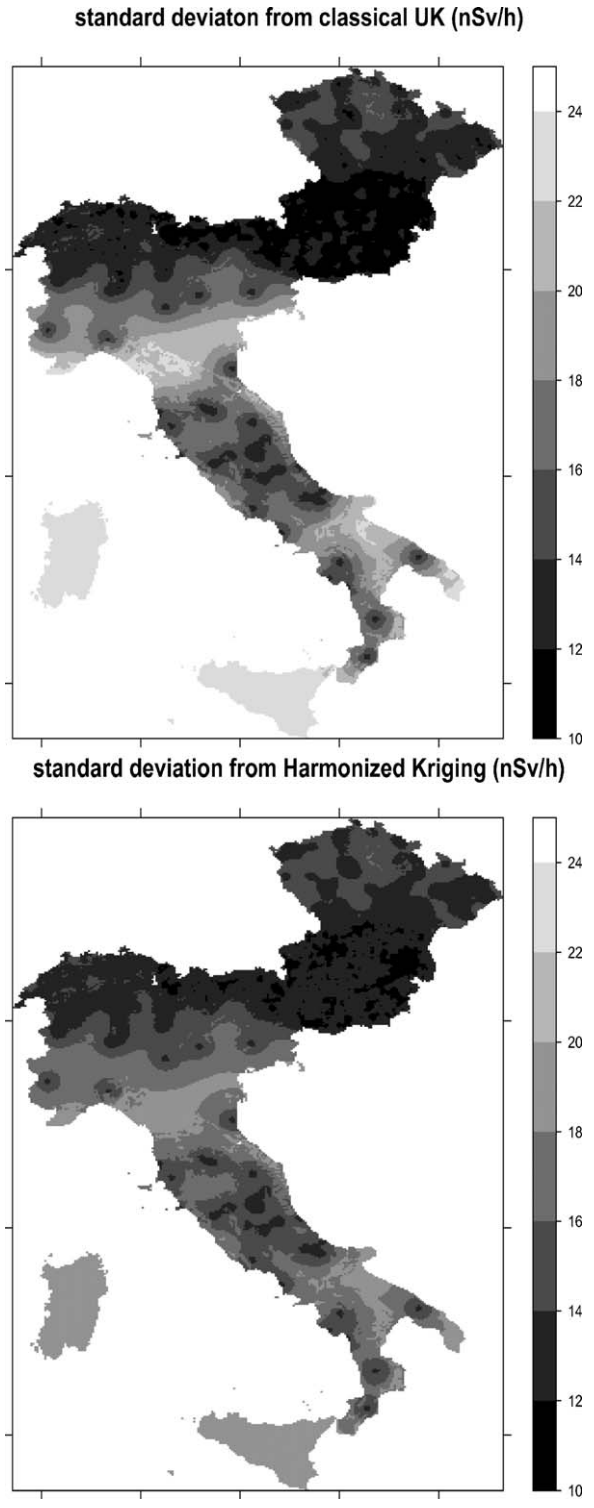

Fig. 6. Gamma dose rate (GDR) from EURDEP data (monthly average in December 2006): standard deviation of Classical UK (top) and Harmonized Kriging (bottom) in nSv/h.

Table 1 presents comparative results for estimation of the drift components. Estimates for country biases and soil drift were constrained to sum to zero so that the intercepts can be easily compared. Only small differences were found between the estimates for

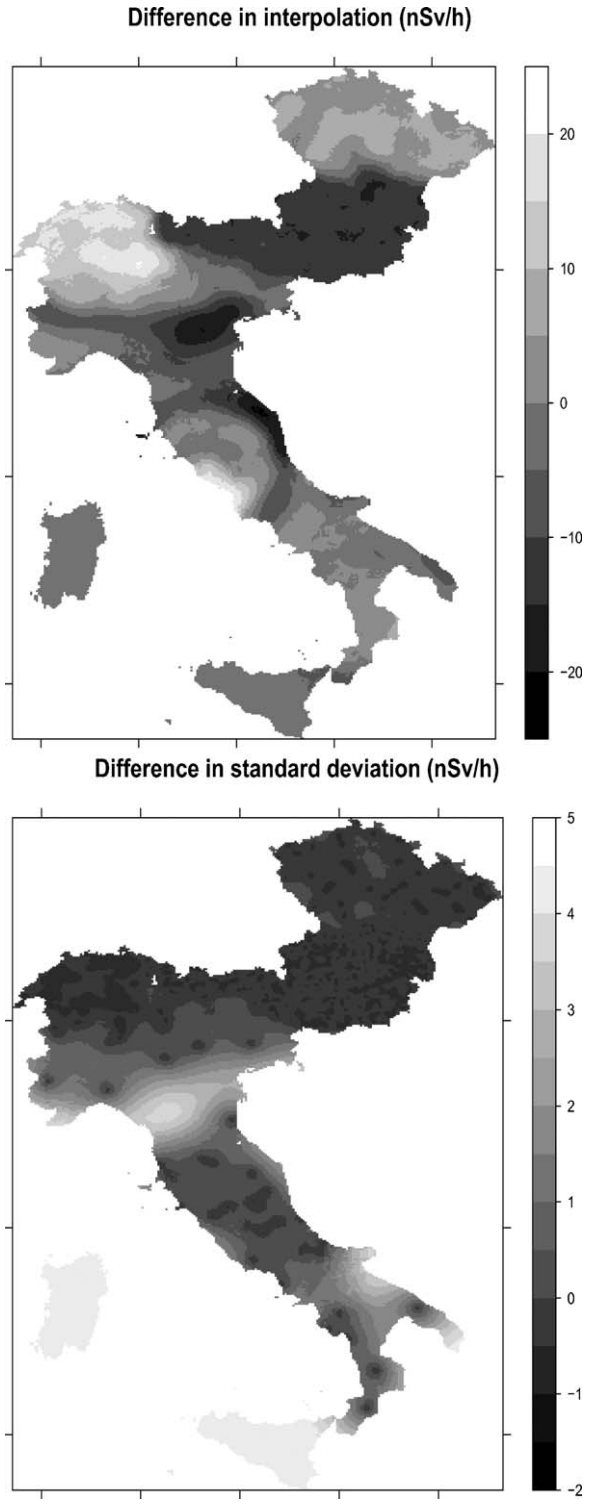

Fig. 7. Gamma dose rate (GDR) from EURDEP data (monthly average in December 2006): differences between Classical UK and Harmonized Kriging interpolated values (top) and kriging error standard deviation (bottom) in nSv/h.

soil drifts with Classical UK versus Harmonized Kriging. The 'detrital formations' soil type was an exception to this tendency, but coefficients estimated from very few samples (i.e. clayey materials, detrital formations, and the other rock category) have large estimation variances. The intercept in the classical model is defined as the mean of estimated drifts and therefore has zero associated standard deviation. In general, highly represented country or soil classes led to smaller standard deviations in the estimates.

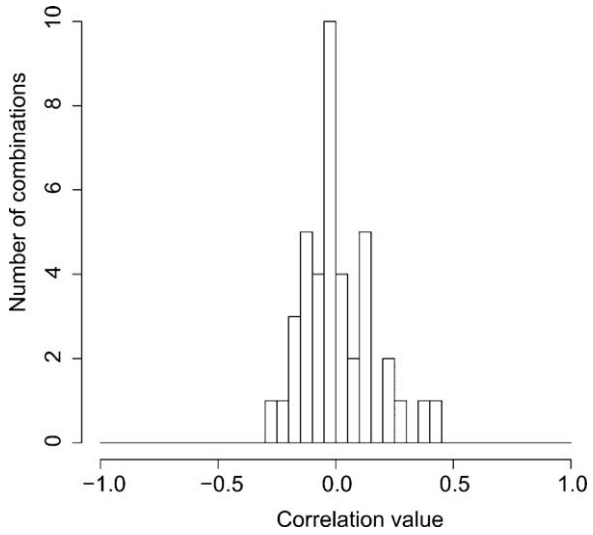

Fig. 8. Correlation histogram of country membership against soil type. The total number of combinations is 40: four countries by 10 soil types.

Maps of kriging predictions and kriging standard deviations are shown in Figs. 5 and 6, respectively. Comparing prediction maps and examining the border region between two countries more closely (e.g., the enlarged region between AT and CZ in Fig. 5), we see that harmonization led to a more gradual transition. In this region, elevation drift appears to have had only a minor effect on the results. The kriging standard deviation maps show the familiar pattern of small values near observation points and in densely sampled areas (see Fig. 1), whereas larger values are obtained in regions where the sampling density is low and at the boundaries of the study area (e.g. the Italian islands).

5.1. Interpretation of the results

In Table 1, relatively small differences are observed between the estimates for soil drift using the Classical UK and Harmonized Kriging methods, indicating modest interaction between country membership and soil type. Fig. 8 shows a histogram of Pearson correlation coefficients for all combinations of the four country codes and 10 soil types. These correlation coefficients were computed considering each category as a binary variable, yielding 40 correlations in total. The largest correlation coefficient (0.41) conveys that most measurements of alluvial soils are located in Switzerland. Hence the Swiss membership bias estimate will be modestly correlated with that of alluvial soils.

In most cases, correlation values between soil types and country memberships were small which means that estimation of country bias had little interference with estimation of soil drift coefficients. Note that in both models (Classical UK and Harmonized Kriging), the influence rank of different soil types remained unchanged (see Table 1). For instance, the largest contribution of soil characteristics to radioactivity exposure appears in volcanic regions, while the smallest contribution corresponds to clayey areas.

When we relied on a model that included soil class and the influence of elevation, we can clearly see the benefit of Harmonized Kriging. The detailed map at the Austrian–Czech border (see right panels in Fig. 5) shows that Harmonized Kriging led to a smoother transition (bottom map) than Classical UK (top map) between the two countries. This is as expected because soil properties remain unchanged and elevation does not change abruptly at the border (see both soil and elevation maps in Fig. 1).

Table 2
Comparison of drift and country bias estimates when omitting the elevation drift in the GDR model (Eq. (25)) – *n* stands for the number of measurements in each class.

	With elevation		Without elevation		*n*
	Estimate	Std. dev.	Estimate	Std. dev.	
Austria (AT)	−17.5	3.2	−18.1	2.8	329
Switzerland (CH)	8.9	4.1	15.5	3.6	53
Czech Republic (CZ)	7.2	3.9	4.9	3.4	53
Italy (IT)	1.4	3.7	−2.3	3.4	36
Water surface and glacier	−2.1	3.9	1.0	3.7	23
Alluvial deposits	2.1	2.6	−0.4	2.4	94
Calcareous rocks	−0.6	2.7	0.4	2.6	80
Clayey materials	−20.6	8.7	−23.0	8.1	4
Sandy materials	−6.4	5.9	−5.2	5.4	11
Loamy materials	4.4	2.5	3.8	2.4	113
Detrital formations	5.7	9.3	0.9	9.1	3
Crystalline rocks	9.3	2.6	13.0	2.5	109
Volcanic rocks	10.6	3.5	10.9	3.4	31
Other rocks	−2.3	8.8	−1.4	8.5	3
Intercept	72.0	2.9	110.8	2.6	471

In order to examine the benefits of harmonization more closely, we mapped the difference in interpolation values between Classical UK and Harmonized Kriging as well as the difference in their standard deviations in Fig. 7. When the network is dense as in Austria, the difference between Classical UK and Harmonized Kriging reflects estimation of the country bias. Conversely, for a country with a sparse network such as Italy the difference may vary from positive to negative values. In this case residuals take a prominent part in the interpolation results, and indeed the variograms of the residuals differed markedly between Classical UK and Harmonized Kriging.

Differences in standard deviations (SD) bear a different spatial structure. SD for Harmonized Kriging was larger in densely monitored zones (Fig. 7, bottom) because the nugget component had a larger influence in the Harmonized Kriging case (Fig. 4). The largest decrease in SD was found in areas with a sparse network of measurements (e.g. continental Italy). Here, reductions in SD resulted from a lower sill in the Harmonized Kriging residual variogram.

5.2. Multicollinearity and interpretation of country biases

If drift components are strongly correlated (nearly collinear in feature space), estimation of associated regression coefficients are subject to convergence problems (Myers et al., 2002). Normally, this has little effect on prediction when all drift components are included in the predictions. However, in the harmonization procedure biases are removed from the predictions and estimation errors are no longer compensated by correlated estimation errors of natural drift coefficients. Hence, multicollinearity may lead to large prediction errors in a harmonization context.

In the GDR prediction example, small correlation coefficients between country membership and soil type (see the above section) led to minor shifts in drift estimates between Classical UK and Harmonized Kriging. However, the effect of multicollinearity may be more substantial in other applications. Thus multicollinearity should be diagnosed and carefully dealt with in harmonization studies.

Evidently, one of the risks of harmonization is that a natural drift may be interpreted as a bias, more specifically in the case where the original UK model is not reliable. Table 2 illustrates this possibility, which becomes apparent when estimates for soil drifts are compared in harmonized GDR models (Eq. (25)) with and without elevation.

When we deliberately simplified the model by excluding the influence of elevation, the fraction of variability in GDR that should actually be related to elevation was redistributed to country bias and soil drift (Table 2). The largest discrepancies between drift estimates were found for variables that were correlated with elevation. For instance, in the estimation of country biases, we can observe the largest difference in Switzerland, a country with extreme variability in elevation. Smaller discrepancies were found in estimates for soil drift categories typically located at low elevations (e.g. clay), whereas higher biases were found for soil types at high elevations (e.g. crystalline rocks). When elevation was omitted from the model, the intercept increased by almost 40 nSv/h. This number roughly corresponds to the mean value for elevation drift in all four countries.

The comparison between the full model and a deliberately simplified or "blinded" model illustrates the importance, particularly in a harmonization context, of a model that includes all of the major natural drifts that describe the state variable. A deficient functional model form can lead to an incorrect harmonization procedure because bias may be grossly under- or overestimated if correlated natural drifts are not included in the model.

6. Discussion and conclusion

In this paper we presented a universal kriging approach that is able to deal with the issue of merging data from different monitoring networks. We propose a model that includes a state equation describing the linear relationship between the state variable and its covariates. We include a measurement equation that describes how measurements depend on the state variable and on measurement errors. In a harmonization context, both systematic and random errors must be considered and included in a geostatistical model. Under this model, the systematic errors are estimated and the state variable is predicted using slight modifications to the universal kriging algorithm. We applied the methodology in an example involving gamma dose rate (GDR) measurements from four European countries to remove bias due to country membership. Results showed that the method worked well and led to more accurate predictions, with less abrupt changes at country boundaries. The harmonization of data in this real case application (i.e., using country membership as a bias factor) worked well and has practical significance for estimation of the physical model as well. However, the performance of the method is influenced by the level of multicollinearity between components in the model. An intuitive approach is to minimize multicollinearity between trend components by optimally selecting the spatial samples for estimation of the model coefficients (Lesch et al., 1995). Essentially this approach can be viewed as an optimization criterion for universal kriging as well (Brus and Heuvelink, 2007). Another approach to the multi-

collinearity problem is to perform a two-staged sampling design optimization procedure, as suggested for instance by Lophaven (2004, Appendix E). Lophaven's two-stage strategy consists of first selecting the best samples for trend estimation, and then adding new samples for estimation of the covariance structure.

If sampling design optimization does not substantially decrease multicollinearity, an alternative approach relies on more local methods of estimation. Skøien et al. (2009) developed a method for detecting biases along boundaries between regions or countries. The method makes use of line kriging, which estimates the average of the target variable along the country border. Line kriging is done twice, each time using observations from one country only. The difference between the two estimates is then used to assess the systematic difference between the networks. The method focuses only on differences between regions and can be advantageous when there is strong multicollinearity between natural and artificial drifts. It avoids this problem by operating at a local scale, where natural drifts are sufficiently constant and their influence can be ignored. The advantage of our method is that it provides a solution that integrates the estimation of bias factors and natural drifts in a universal kriging approach.

The harmonization model presented in this work also assumes that the relationships between covariates and the state variable, and between bias factors and the state variable, are linear. This assumption greatly simplifies the statistical analysis, although it may be too simplistic for some real-world applications. A simple extension would be to consider appropriate transformations of covariates and bias factors prior to statistical modelling. A more elaborate approach would be to apply a generalized linear model for geostatistical data (Diggle and Ribeiro, 2007), which would also be able to handle non-normality of residuals.

Two main developments in harmonization methods are envisaged. First, because biases between networks are linked to calibration issues, comparison studies between different device types are necessary to derive calibration models that include a proportional effect (Osborne, 1991). The Harmonized Kriging approach can be modified to handle proportional effects as in Fassò et al. (2007). This should further generalize the model, making the approach more complete. The second anticipated development relies on the use of prior information about the biases. If expert knowledge or more relevant bias estimates are available, these can be included as priors in a Bayesian approach (Diggle and Ribeiro, 2007).

Bias correction is increasingly important because globalization leads to increased integration of various datasets for statistical analysis. For instance, the establishment of European soil property maps confronts the same problem (Carré et al., 2008). We believe that geostatistical bias correction methods can provide the necessary harmonization procedures, but a number of issues need further attention before these methods are ready for routine use.

Acknowledgements

This work was funded by the European Commission, under the Sixth Framework Programme, Contract No. 033811, with the DG INFSO, action Line IST-2005-2.5.12 ICT for Environmental Risk Management. The views expressed herein are those of the authors and are not necessarily those of the European Commission. We thank two anonymous reviewers for their valuable comments.

References

Armstrong, M., 1984. Problems with universal kriging. Journal of Mathematical Geology 16 (1), 101–108.
Bartholomeus, R.P., Witte, J.P.M., van Bodegom, P.M., Aerts, R., 2008. The need of data harmonization to derive robust empirical relationships between soil conditions and vegetation. Journal of Vegetation Science 19, 799–808.
Bossew, P., De Cort, M., Dubois, G., Stöhlker, U., Tollefsen, T., Wätjen, U., 2008. AIRDOS, evaluation of existing standards of measurement of ambient dose rate; and of sampling, sample preparation and measurement for estimating radioactivity levels in air. Tech. Rep. TREN/NUCL/S12.378241 ref. 21894–2004-04 A1CO ISP BE, European Joint Research Center, Ispra, Italy.
Brus, D.J., Heuvelink, G.B.M., 2007. Optimization of sample patterns for universal kriging of environmental variables. Geoderma 138, 86–95.
Carré, F., Jeannée, N., Casalegno, S., Lemarchand, O., Reuter, H.I., Montanarella, L., 2008. Mapping the CN ratio of the forest litters in Europe – lessons for global DSM. In: Logan2008. Salt Lake City, United States.
Chilès, J.-P., Delfiner, P., 1999. Geostatistics: Modeling Spatial Uncertainty. Wiley & Sons, New York.
Christensen, R., 1991. Linear Models for Multivariate, Time Series, and Spatial Data. Springer Texts in Statistics. Springer-Verlag, New York.
Cressie, N., 1993. Statistics for Spatial Data. Wiley Series in Probability and Mathematical Statistics. Wiley & Sons, New York.
De Cort, M., De Vries, G., 1997. The European Union Radiological Data Exchange Platform (EURDEP): two years of international data exchange experience. Radiation Protection Dosimetry 73, 17–20.
Diggle, P.J., Ribeiro Jr., P.J., 2007. Model-based Geostatistics. Springer, New York.
Fassò, A., Cameletti, M., Nicolis, O., 2007. Air quality monitoring using heterogeneous networks. Environmetrics 18, 245–264.
Gego, E.L., Porter, P.S., Irwin, J.S., Hogrefe, C., Rao, S.T., 2005. Assessing the comparability of ammonium, nitrate and sulfate concentrations measured by three air quality monitoring networks. Pure and Applied Geophysics 162 (10), 1919–1939.
Gold, S., Korotkov, A.V., Sasse, V., 2006. The development of European forest resources, 1950 to 2000. Forest Policy and Economics 8, 183–192.
Herold, M., Woodcock, C.E., Di Gregario, A., Mayaux, P., Belward, A.S., Latham, J., Schumullius, C.C., 2006. A joint initiative for harmonization and validation of land cover datasets. IEEE Transactions on Geoscience and Remote Sensing 44 (7), 1719–1727.
Hiemstra, P.H., Pebesma, E.J., Twenhöfel, C.J.W., Heuvelink, G.B.M., 2009. Real-time automatic interpolation of ambient gamma dose rates from the Dutch radioactivity monitoring network. Computers & Geosciences 35, 1711–1721.
Köhl, M., Traub, B., Päivinen, R., 2000. Harmonization and standardization in multi-national environmental statistics – mission impossible? Environmental Monitoring and Assessment 63, 361–380.
Kovitz, J.L., Christakos, G., 2004. Spatial statistics of clustered data. Stochastic Environmental Research 18, 147–166.
Lesch, S.M., Strauss, D.J., Rhoades, J.D., 1995. Spatial prediction of soil salinity using electromagnetic induction techniques 2. An efficient spatial sampling algorithm suitable for multiple linear regression model identification and estimation. Water Resources Research 31 (2), 387–398.
Lophaven S., 2004. Design and analysis of environmental monitoring programs. Ph.D. thesis, Technical University of Denmark.
Marcotte, D., 1995. Conditional simulation with data subject to measurement error: post-simulation filtering with modified factorial kriging. Mathematical Geology 27 (6), 749–762.
Myers, R.H., Montgomery, D.C., Vining, G.C., 2002. Generalyzed Linear Models. Wiley Series in Probability and Statistics, New York.
Osborne, C., 1991. Statistical calibration: a review. International Statistical Review 59 (3), 309–336.
Otuama, E., Hamre, M., 2007. Design and implementation of a distributed GIS portal for oil spill and harmful algal bloom monitoring in the marine environment. Marine Geodesy 30, 145–168.
Parr, T.W., Ferretti, M., Simpson, I.C., Forsius, M., Kovács-Láng, E., 2002. Towards a long term integrated monitoring program in Europe: network design in theory and practice. Environmental Monitoring and Assessment 78, 253–290.
Prechtel, A., von Lützow, M., Schneider, B.U., Bens, O., Bannick, C.G., Kögel-Knabner, I., Hüttl, R.F., 2009. Organic carbon in soils of Germany: Status quo and the need for new data to evaluate potentials and trends of soil carbon sequestration. Journal of Plant Nutrition and Soil Science 172, 601–614.
Rivoirard, J., Simmonds, J., Foote, K., Fernandes, P., Bez, N., 2000. Geostatistics for Estimating Fish Abundance. Blackwell Science, Oxford, UK.
Schröder, W., Pesch, R., Schmidt, G., 2006. Identifying and closing gaps in environmental monitoring by means of metadata, ecological regionalization and geostatistics using the UNESCO biosphere reserve Rhoen (Germany) as an example. Environmental Monitoring and Assessment 114, 461–488.
Searle, S.R., 1997. Linear Models. Wiley Classics Library. Wiley & Sons, New York.
Skøien, J.O., Baume, O.P., Pebesma, E.J., Heuvelink, G.B.M., 2009. Identifying and removing heterogeneities between monitoring networks. Environmetrics 24 (1), 66–84.
Suits, D., 1957. Use of dummy variables in regression equations. Journal of the American Statistical Association 52, 548–551.
Szegvary, T., Conen, F., Stöhlker, U., Dubois, G., Bossew, P., de Vries, G., 2007. Mapping terrestrial γ-dose rate in Europe based on routine monitoring data. Radiation Measurements 42, 1531–1572.
Wagner, G., Desaules, A., Muntau, H., Theocharopoulos, S., Quevauviller, P., 2001. Harmonisation and quality assurance in pre-analytical steps of soil contamination studies – conclusions and recommendations of CEEM Soil project. The Science of the Total Environment 264, 103–117.
Wissmann, F., Rupp, A., Stöhlker, U., 2007. Characterization of dose rate instruments for environmental radiation monitoring. Kerntechnik 72 (4), 193–198.
Zähringer, M., Sempau, J., 1996. The assessment of the representativeness of data from dose rate monitoring stations. Radiation Protection Dosimetry 64 (4), 275–282.